Black Strings, Low Viscosity Fluids, and Violation of Cosmic Censorship

Luis Lehner[1,2,3] and Frans Pretorius[4]

[1]*Perimeter Institute for Theoretical Physics, Waterloo, Ontario N2L 2Y5, Canada*
[2]*Department of Physics, University of Guelph, Guelph, Ontario N1G 2W1, Canada*
[3]*Canadian Institute For Advanced Research (CIFAR), Cosmology and Gravity Program, Canada*
[4]*Department of Physics, Princeton University, Princeton, New Jersey 08544, USA*

(Received 11 July 2010; published 2 September 2010; corrected 8 November 2010)

We describe the behavior of 5-dimensional black strings, subject to the Gregory-Laflamme instability. Beyond the linear level, the evolving strings exhibit a rich dynamics, where at intermediate stages the horizon can be described as a sequence of 3-dimensional spherical black holes joined by black string segments. These segments are themselves subject to a Gregory-Laflamme instability, resulting in a self-similar cascade, where ever-smaller satellite black holes form connected by ever-thinner string segments. This behavior is akin to satellite formation in low-viscosity fluid streams subject to the Rayleigh-Plateau instability. The simulation results imply that the string segments will reach zero radius in finite asymptotic time, whence the classical space-time terminates in a naked singularity. Since no fine-tuning is required to excite the instability, this constitutes a generic violation of cosmic censorship.

DOI: 10.1103/PhysRevLett.105.101102 PACS numbers: 04.50.Gh, 04.20.−q, 04.25.D−

Introduction.—While stationary black holes in 4 space-time dimensions (4D) are stable to perturbations, higher dimensional analogues are not. Indeed, as first illustrated by Gregory and Laflamme in the early 1990s [1], black strings and p-branes are linearly unstable to long wavelength perturbations in 5 and higher dimensions. Since then, a number of interesting black objects in higher dimensional gravity have been discovered, many of them exhibiting similar instabilities (see, e.g., [2]).

An open question for all unstable black objects is what the end state of the perturbed system is. For black strings, the authors of Ref. [1] conjectured that the instability would cause the horizon to pinch-off at periodic intervals, giving rise to a sequence of black holes. One reason for this conjecture comes from entropic considerations: For a given mass per unit length and periodic spacing above a critical wavelength λ_c, a sequence of hyperspherical black holes has higher entropy than the corresponding black string. Classically, event horizons cannot bifurcate without the appearance of a naked singularity [3]. Thus, reaching the conjectured end state would constitute a violation of cosmic censorship, without ''unnatural'' initial conditions or fine-tuning, and be an example of a classical system evolving to a regime where quantum gravity is required.

This conjecture was essentially taken for granted until several years later when it was proved that the generators of the horizon can not pinch-off in finite affine time [4]. From this, it was conjectured that a new, nonuniform black string end state would be reached [4]. Subsequently, stationary, nonuniform black string solutions were found [5,6]; however, they had less entropy than the uniform string and so could not be the putative new end state, at least for dimensions lower than 13 [7].

A full numerical investigation studied the system beyond the linear regime [8], though not far enough to elucidate the end state before the code ''crashed.'' At that point the horizon resembled spherical black holes connected by black strings, though no definitive trends could be extracted, still allowing for both conjectured possibilities: (a) a pinch-off in infinite affine time, (b) evolving to a new, nonuniform state. If (a), a question arises whether pinch-off happens in infinite *asymptotic* time; if so, any bifurcation would never be seen by outside observers, and cosmic censorship would hold. While this might be a natural conclusion, it was pointed out in Refs. [9,10] that, due to the exponentially diverging rate between affine time and a well-behaved asymptotic time, pinch-off could occur in finite asymptotic time.

A further body of (anecdotal) evidence supporting the Gregory-Laflamme (GL) conjecture comes from the striking resemblance of the equations governing black hole horizons to those describing fluid flows, the latter of which do exhibit instabilities that often result in breakup of the fluid. The fluid-horizon connection harkens back to the membrane paradigm [11], and also in more recently developed correspondences [12,13]. In [14] it was shown that the dispersion relation of Rayleigh-Plateau unstable modes in hypercylindrical fluid flow with tension agreed well with those of the GL modes of a black string. Similar behavior was found for instabilities of a self-gravitating cylinder of fluid in Newtonian gravity [15]. In [16], by using a perturbative expansion of the Einstein field equations [13] to relate the dynamics of the horizon to that of a viscous fluid, the GL dispersion relation was *derived* to a good approximation, thus going one step further than showing analogous behavior between fluids and horizons.

What is particularly intriguing about fluid analogies, and what they might imply about the black string case, is that breakup of an unstable flow is preceded by formation of spheres separated by thin necks. For high-viscosity liquids,

a single neck forms before breakup. For lower-viscosity fluids, smaller "satellite" spheres can form in the necks, with more generations forming the lower the viscosity (see [17] for a review). In the membrane paradigm, black holes have a lower shear viscosity to entropy ratio than any known fluid [18].

Here we revisit the evolution of 5D black strings by using a new code. This allows us to follow the evolution well beyond the earlier study [8]. We find that the dynamics of the horizon unfolds as predicted by the low-viscosity fluid analogues: The string initially evolves to a configuration resembling a hyperspherical black hole connected by thin string segments; the string segments are themselves unstable, and the pattern repeats in a self-similar manner to ever-smaller scales. Because of finite computational resources, we cannot follow the dynamics indefinitely. If the self-similar cascade continues as suggested by the simulations, arbitrarily small length scales, and in consequence arbitrarily large curvatures, will be revealed outside the horizon in finite asymptotic time.

Numerical approach.—We solve the vacuum Einstein field equations in a 5-dimensional (5D) asymptotically flat space-time with an $SO(3)$ symmetry. Since perturbations of 5D black strings violating this symmetry are stable and decay [1], we do not expect that imposing this symmetry qualitatively affects the results presented here.

We use the generalized harmonic formulation of the field equations [19] and adopt a Cartesian coordinate system related to spherical polar coordinates via $\bar{x}^i = (\bar{t}, \bar{x}, \bar{y}, \bar{z}, \bar{w}) = (t, r\cos\phi\sin\theta, r\sin\phi\sin\theta, r\cos\theta, z)$. The black string horizon has topology $S^2 \times R$; (θ, ϕ) are coordinates on the 2-sphere, and z ($\bar{w}$) is the coordinate in the string direction, which we make periodic with length L. We impose a Cartesian harmonic gauge condition, i.e., $\nabla_\alpha \nabla^\alpha \bar{x}^i = 0$, as empirically this seems to result in more stable numerical evolution compared to spherical harmonic coordinates. The $SO(3)$ symmetry is enforced by using the variant of the "cartoon" method [20] described in [19], where we evolve only a $\bar{y} = \bar{z} = 0$ slice of the space-time. We further add constraint damping [21], which introduces two parameters κ and ρ; we use $(\kappa, \rho = 1, -0.5)$, where a nonzero ρ is essential to damp an unstable zero-wavelength mode arising in the z direction.

We discretize the equations by using 4th-order finite difference approximations and integrate in time by using 4th-order Runge-Kutta. To resolve the small length scales that develop during evolution, we use Berger and Oliger adaptive mesh refinement. Truncation error estimates are used to dynamically generate the mesh hierarchy, and we use a spatial and temporal refinement ratio of 2.

At the outer boundary we impose Dirichlet conditions, with the metric set to that of the initial data. These conditions are not strictly physically correct at finite radius, though the outer boundary is placed sufficiently far that it is causally disconnected from the horizon for the time of the simulation. We use black hole excision on the inner surface; namely, we find the apparent horizon (AH) by using a flow method and dynamically adjust this boundary (the excision surface) to be some distance within the AH. Because of the causal nature of space-time inside the AH, no boundary conditions are placed on the excision surface.

We adopt initial data describing a perturbed black string of mass per unit length M and length $L = 20M \approx 1.4L_c$ (L_c is the critical length above which all perturbations are unstable). These data were used in [8], and we refer the reader to that work for further details.

We evaluate the following curvature scalars on the AH:

$$K = IR_{\rm AH}^4/12, \qquad S = 27(12J^2I^{-3} - 1) + 1, \qquad (1)$$

where $I = R_{abcd}R^{abcd}$, $J = R_{abcd}R^{cdef}R_{ef}{}^{ab}$, and $R_{\rm AH}$ is the areal radius of the AH at the corresponding point. K and S have been scaled to evaluate to $\{6, 1\}$ for the hyperspherical black hole and black string, respectively.

Results.—The results described here are from simulations where the computational domain is $(r, z) \in ([0, 320M] \times [0, 20M])$. The coarsest grid covering the entire domain has a resolution of $(N_r, N_z) = (1025, 9)$ points. For convergence studies we ran simulations with 3 values of the maximum estimated truncation error τ: ["low", "medium", and "high"] resolution have $\tau = [\tau_0, \tau_0/8, \tau_0/64]$, respectively. This leads to an initial hierarchy where the horizon of the black string is covered by 4, 5, and 6 additional refined levels for the low to high resolutions, respectively. Each simulation was stopped when the estimated computational resources required for continued evolution were prohibitively high (which naturally occurred later in physical time for the lower resolutions); by then the hierarchies were as deep as 17 levels.

Figure 1 shows the integrated AH area A within $z \in [0, L]$ versus time. At the end of the lowest resolution run, the total area is $A = (1.369 \pm 0.005)A_0$ [22], where A_0 is the initial area; interestingly, this almost reaches the value of $1.374A_0$ that an exact 5D black hole of the same total mass would have. Figure 2 shows snapshots of embedding diagrams of the AH, and Fig. 3 shows the curvature invariants evaluated on the AH at the last time step, both from the medium resolution run.

The shape of the AH, and that the invariants are tending to the limits associated with pure black strings or black holes at corresponding locations on the AH, suggests it is reasonable to describe the local geometry as being similar

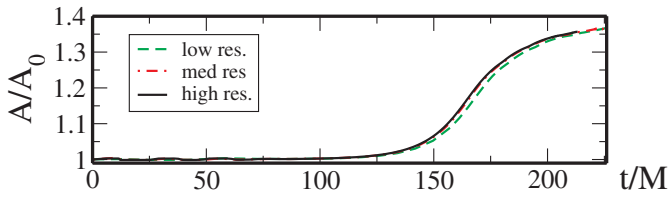

FIG. 1 (color online). (Normalized) apparent horizon area vs time.

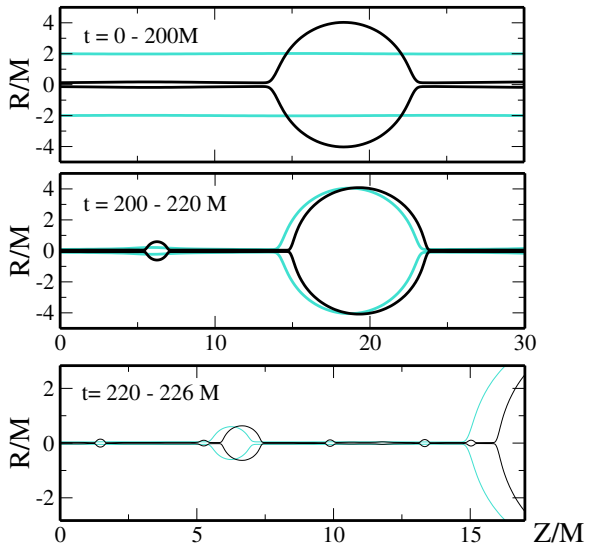

FIG. 2 (color online). Embedding diagram of the apparent horizon at several instances in the evolution of the perturbed black string, from the medium resolution run. R is areal radius, and the embedding coordinate Z is defined so that the proper length of the horizon in the space-time z direction (for a fixed t, θ, ϕ) is exactly equal to the Euclidean length of $R(Z)$ in the above figure. For visual aid, copies of the diagrams reflected about $R = 0$ have also been drawn in. The light (dark) lines denote the first (last) time from the time segment depicted in the corresponding panel. The computational domain is periodic in z with period $\delta z = 20M$; at the initial (final) time of the simulation $\delta Z = 20M$ ($\delta Z = 27.2M$). See [28].

to a sequence of black holes connected by black strings. This also strongly suggests that satellite formation will continue self-similarly, as each string segment resembles a uniform black string that is sufficiently long to be unstable. Even if at some point in the cascade shorter segments were to form, this would not be a stable configuration as generically the satellites will have some nonzero z velocity, causing adjacent satellites to merge and effectively lengthening the connecting string segments. With this interpretation, we summarize key features of the AH dynamics in Table I.

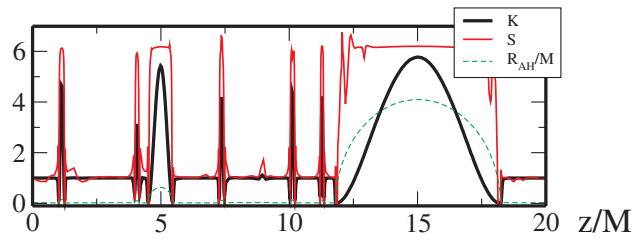

FIG. 3 (color online). Curvature invariants evaluated on the apparent horizon at the last time of the simulation depicted in Fig. 2. The invariant K evaluates to 1 for an exact black string and 6 for an exact spherical black hole, similarly for S (1).

We estimate when this self-similar cascade will end. The time when the first satellite appears is controlled by the perturbation imparted by the initial data; here that is $T_0/M \approx 118$. Subsequent time scales should approximately represent the generic development of the instability. The time for the first instability after that sourced by the initial data is $T_1/M \approx 80$. Beyond that, with the caveats that we have a small number of points and poor control over errors at late times, each subsequent instability unfolds on a time scale $X \approx 1/4$ times that of the preceding one. This is to be expected if, as for the exact black string, the time scale is proportional to the string radius. The time t_0 of the end state is then $t_0 \approx T_0 + \sum_{i=0}^{\infty} T_1 X^i = T_0 + T_1/(1 - X)$. For the data here, $t_0/M \approx 231$; then the local string segments reach zero radius, and the curvature visible to exterior observers diverges. Figure 4 shows a few points on the AH, scaled assuming this behavior. In the Rayleigh-Plateau analogue, the shrinking neck of a fluid stream has a self-similar scaling solution that satisfies $r \propto (t_0 - t)$, or $d \ln r/d[-\ln(t_0 - t)] = -1$, where r is the stream radius (see [23], and [24] for extensions to higher dimensions); to within 10%–20%, this is the average slope we see (e.g., Fig. 4) at string segments of the AH at late times.

Conclusions.—We have studied the dynamics of a perturbed, unstable 5D black string. The horizon behaves similarly to the surface of a stream of low-viscosity fluid subject to the Rayleigh-Plateau instability. Multiple generations of spherical satellites, connected by ever-thinner string segments, form. Curvature invariants on the horizon

TABLE I. Properties of the evolving black string apparent horizon, interpreted as proceeding through several self-similar generations, where each local string segment temporarily reaches a near-steady state before the onset of the next GL instability. t_i is the time when the instability has grown to where the nascent spherical region reaches an areal radius 1.5 times the surrounding string-segment radius $R_{s,i}$, which has an estimated proper length $L_{s,i}$ (the critical L/R is ≈ 7.2 [1]). n_s is the number of satellites that form per segment, that each attain a radius $R_{h,f}$ measured at the end of the simulation. Errors, where appropriate, come from convergence tests. After the second generation the number and distribution of satellites that form depend sensitively on grid parameters, and perhaps the only "convergent" result we have then is that at roughly $t = 223$ a third generation *does* develop. We surmise the reason for this is that the long parent string segments could have multiple unstable modes with similar growth rates, and which is first excited is significantly affected by truncation error. We have had only the resources to run the lowest resolution simulation for sufficiently long to see the onset of the 4th generation, hence the lack of error estimates and the presence of question marks in the corresponding row.

Gen.	t_i/M	$R_{s,i}/M$	$L_{s,i}/R_{s,i}$	n_s	$R_{h,f}/M$
1	118.1 ± 0.5	2.00	10.0	1	$4.09 \pm 0.5\%$
2	203.1 ± 0.5	$0.148 \pm 1\%$	$105 \pm 1\%$	1	$0.63 \pm 2\%$
3	223 ± 2	$0.05 \pm 20\%$	$\approx 10^2$	>1	0.1–0.2
4	≈ 227	≈ 0.02	$\approx 10^2$	>1(?)	?

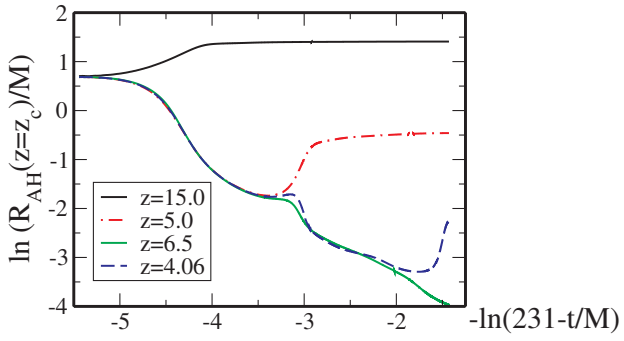

FIG. 4 (color online). Logarithm of the areal radius vs logarithm of time for select points on the apparent horizon from the simulation depicted in Fig. 2. We have shifted the time axis *assuming* self-similar behavior; the putative naked singularity forms at asymptotic time $t/M \approx 231$. The coordinates at $z = 15$, 5, and 4.06 correspond to the maxima of the areal radii of the first and second generation satellites and one of the third generation satellites at the time the simulation stopped. The value $z = 6.5$ is a representative slice in the middle of a piece of the horizon that remains stringlike throughout the evolution.

suggest that this is a self-similar process, where at each stage the local string or spherical segments resemble the corresponding exact solutions. Furthermore, the time scale for the formation of the next generation is proportional to the local string radius, implying the cascade will terminate in finite asymptotic time. Since local curvature scalars grow with inverse powers of the string radius, this end state will thus be a naked, curvature singularity. If quantum gravity resolves these singularities, a series of spherical black holes will emerge. However, small momentum perturbations in the extra dimension would induce the merger of these black holes; thus, for a compact extra dimension the end state of the GL instability will be a single black hole with spherical topology.

The kind of singularity reached here via a self-similar process is akin to that formed in critical gravitational collapse [25]; however, here no fine-tuning is required. Thus, 5 (and presumably higher) -dimensional Einstein gravity allows solutions that generically violate cosmic censorship. Angular momentum will likely not alter this conclusion, since as argued in [13], and shown in [26], rotation does not suppress the unstable modes and, moreover, induces superradiant and gyrating instabilities [27].

We thank V. Cardoso, M. Choptuik, D. Garfinkle, R. Emparan, S. Gubser, G. Horowitz, D. Marolf, R. Myers, W. Unruh, and R. Wald for stimulating discussions. This work was supported by NSERC (L. L.), CIFAR (L. L.), the Alfred P. Sloan Foundation (F. P.), and NSF Grant No. PHY-0745779 (F. P.). Simulations were run on the *Woodhen* cluster at Princeton University and at LONI. Research at Perimeter Institute is supported through Industry Canada and by the Province of Ontario through the Ministry of Research & Innovation.

[1] R. Gregory and R. Laflamme, Phys. Rev. Lett. **70**, 2837 (1993).
[2] R. Emparan and H. S. Reall, Living Rev. Relativity **11**, 6 (2008); T. Harmark, V. Niarchos, and N. A. Obers, Classical Quantum Gravity **24**, R1 (2007); B. Kol, Phys. Rep. **422**, 119 (2006).
[3] S. W. Hawking and G. F. R. Ellis, *The Large Scale Structure of Space-Time* (Cambridge University Press, Cambridge, England, 1975).
[4] G. T. Horowitz and K. Maeda, Phys. Rev. Lett. **87**, 131301 (2001).
[5] T. Wiseman, Classical Quantum Gravity **20**, 1137 (2003).
[6] S. S. Gubser, Classical Quantum Gravity **19**, 4825 (2002).
[7] E. Sorkin, Phys. Rev. Lett. **93**, 031601 (2004).
[8] M. W. Choptuik *et al.*, Phys. Rev. D **68**, 044001 (2003).
[9] D. Garfinkle, L. Lehner, and F. Pretorius, Phys. Rev. D **71**, 064009 (2005).
[10] D. Marolf, Phys. Rev. D **71**, 127504 (2005).
[11] K. S. Thorne, R. H. Price, and D. A. Macdonald, *Black Holes: The Membrane Paradigm* (Yale University Press, New Haven, CT, 1986), p. 367.
[12] S. Bhattacharyya, V. E. Hubeny, S. Minwalla, and M. Rangamani, J. High Energy Phys. 02 (2008) 045.
[13] R. Emparan, T. Harmark, V. Niarchos, and N. A. Obers, J. High Energy Phys. 03 (2010) 063.
[14] V. Cardoso and O. J. C. Dias, Phys. Rev. Lett. **96**, 181601 (2006).
[15] V. Cardoso and L. Gualtieri, Classical Quantum Gravity **23**, 7151 (2006).
[16] J. Camps, R. Emparan, and N. Haddad, J. High Energy Phys. 05 (2010) 042.
[17] J. Eggers, Rev. Mod. Phys. **69**, 865 (1997).
[18] P. K. Kovtun, D. T. Son, and A. O. Starinets, Phys. Rev. Lett. **94**, 111601 (2005).
[19] F. Pretorius, Classical Quantum Gravity **22**, 425 (2005).
[20] M. Alcubierre *et al.*, Int. J. Mod. Phys. D **10**, 273 (2001).
[21] C. Gundlach, J. M. Martin-Garcia, G. Calabrese, and I. Hinder, Classical Quantum Gravity **22**, 3767 (2005).
[22] The error in the area was estimated from convergence at the latest time data were available from all simulations.
[23] J. Eggers, Phys. Rev. Lett. **71**, 3458 (1993).
[24] U. Miyamoto, arXiv:1007.4302; (to be published).
[25] M. W. Choptuik, Phys. Rev. Lett. **70**, 9 (1993).
[26] O. J. C. Dias, P. Figueras, R. Monteiro, H. S. Reall, and J. E. Santos, J. High Energy Phys. 05 (2010) 076.
[27] D. Marolf and B. Cabrera Palmer, Phys. Rev. D **70**, 084045 (2004); V. Cardoso and J. P. S. Lemos, Phys. Lett. B **621**, 219 (2005); V. Cardoso and S. Yoshida, J. High Energy Phys. 07 (2005) 009.
[28] See supplementary material at http://link.aps.org/supplemental/10.1103/PhysRevLett.105.101102 for a movie of the low resolution run data.